Preparation, crystal structures and electrical properties of PF$_6$ and AsF$_6$ salts of a novel furopyrazine-extended donor (BDTFP) with a two-leg ladder type orbital overlapping mode

Toshihiro Ise,[a] Takehiko Mori[b] and Kazuko Takahashi*[c]

[a]Department of Chemistry, Graduate School of Science, Tohoku University, Sendai 980-8578, Japan
[b]Department of Organic and Polymeric Materials, Tokyo Institute of Technology, O-okayama, Tokyo, 152-8552, Japan
[c]Center for Interdisciplinary Research, Tohoku University, Sendai 980-8578, Japan.
E-mail: tkazuko@cir.tohoku.ac.jp

A novel electron donor BDTFP has been synthesized and it is demonstrated that PF$_6$ and AsF$_6$ cation radical salts of BDTFP undergo phase transitions at 175 and 220 K, respectively and have a very unusual two-leg ladder type intermolecular overlapping mode in their crystal structures.

Creation of new and superior π-donors is necessary to ensure versatile development in the field of organic conductors. Conjugation-extended TTF analogues with an appropriate π-linking group between the 1,3-dithiole rings of TTF[1] are promising for achieving high conductivity by reducing the on-site Coulombic repulsion and for obtaining high T_c organic superconductors by increasing the thickness of the effective conducting layer.[2] We have synthesized 2,5-bis(1,3-dithiol-2-ylidene)-2,5-dihydrothiophene (BDTT) and its chalcogeno derivatives.[3] However, crystal growth of their radical cation salts was difficult since they are somewhat air-sensitive in solution owing to their high electron donating abilities. The electron donating ability might be weakened by introduction of

BDTFP **1**
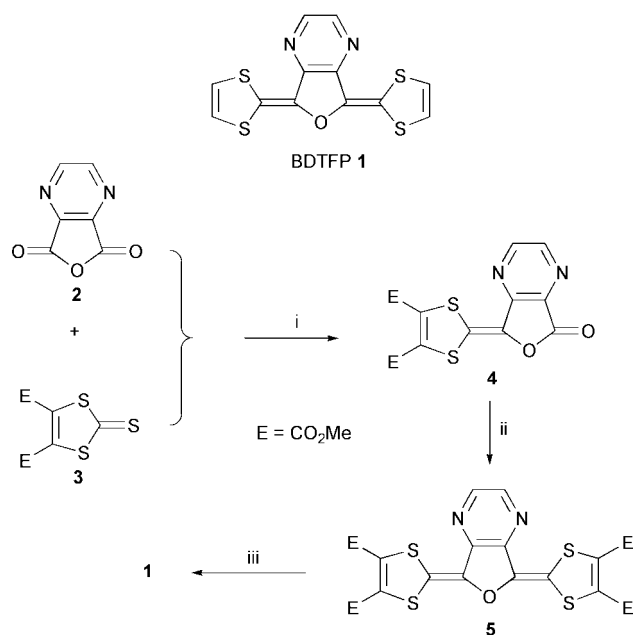
Scheme 1 *Reagents and conditions*: i, P(OMe)$_3$, toluene, reflux, 3 h, 44%; ii, **3**, P(OMe)$_3$, 90 °C, 3 h, 94%; iii, LiBr·H$_2$O, HMPA, 90 °C, 1 h, then 155 °C, 1 h; quantitative yield.
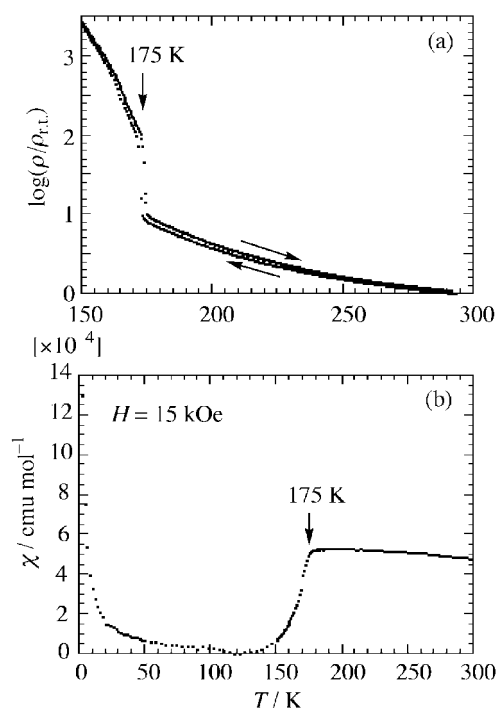

Fig. 1 (a) Temperature dependence of the normalized resistivity and (b) temperature dependence of the static magnetic susceptibility of [BDTFP]$_2$[PF$_6$][PhCl]$_{0.5}$.

an electron deficient pyrazine ring.[4] With this in mind, we have now designed and synthesized 5,7-bis(1,3-dithiol-2-ylidene)-5,7-dihydrofuro[3,4-*b*]pyrazine (BDTFP) **1** as a new type of extended donor. We have obtained single crystalline PF$_6$ and AsF$_6$ salts of BDTFP and have clarified crystal structures, and conducting and magnetic properties of these salts revealing that these salts undergo phase transitions at 175 or 220 K and have a very unusual two-leg ladder type intermolecular orbital overlapping mode. This is the first example of a detailed investigation on the radical cation salts of pyrazine fused conjugation-extended donors.

BDTFP was synthesized starting from the anhydride **2**[5] according to the routes shown in Scheme 1.† BDTFP is oxidized reversibly in two successive one-electron transfer reactions to give stable cation radical and dication species and this is demonstrated by the cyclic voltammogram which
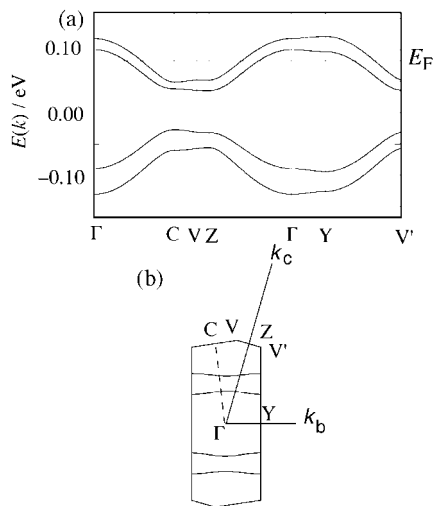
DOI: 10.1039/b008758k

Fig. 2 (a) Band structure and (b) Fermi surface of [BDTFP]₂[PF₆][PhCl]₀.₅, calculated by the tight binding approximation method.
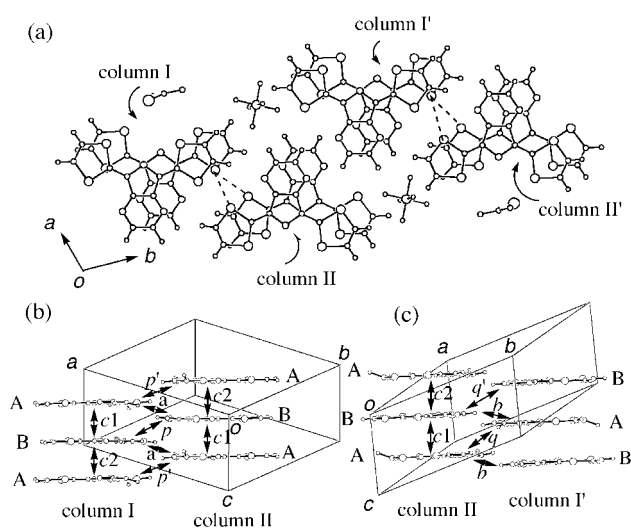

Fig. 3 Crystal structure of [BDTFP]₂[PF₆][PhCl]₀.₅: (a) projection onto the *ab*-plane showing the ladder type structure, (b) overlap mode between columns I and II, (c) overlap mode between columns II and I'.
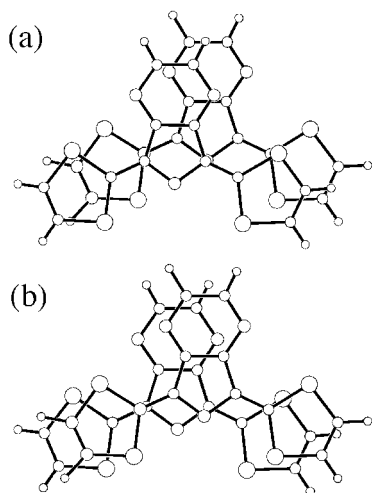

Fig. 4 Overlapping modes of BDTFP molecules in [BDTFP]₂[PF₆][PhCl]₀.₅: (a) Intra-dimer overlap, *c*1; (b) Inter-dimer overlap, *c*2.

Table 1 Intermolecular overlap integrals ($S \times 10^3$) in [BDTFP]₂[PF₆][PhCl]₀.₅^a

Intra-column		Column I–II		Column II–I'	
$c1$	−7.5	a	−0.39	b	−0.20
$c2$	−3.4	p	2.5	q	0.070
		p'	0.38	q'	0.0

^{a}The overlap integrals between neighboring molecules are calculated by the extended Hückel method using X-ray crystal structures and the π–HOMO coefficients of molecules A and B calculated by MNDO-PM3 method. The overlap directions are indicated in Fig. 3.

exhibits two pairs of single-electron redox waves at half-wave oxidation potentials of +0.36 and +0.62 V (*vs.* SCE in PhCN at 25 °C). The first oxidation potential is more positive by 0.25 V than that of BDTT (+0.11 V), reflecting the stabilization of the energy level of the HOMO by the annelation of the electron-deficient pyrazine ring.

BDTFP formed a 1:1 TCNQ complex exhibiting a room temperature conductivity (σ_{rt}) of 20 S cm^{-1} measured on a compressed pellet. The TCNQ complex is considered to be metallic from room temperature down to 150 K since the Arrhenius plot of temperature dependence of the resistivity is not linear in this region and the Pauli-like paramagnetic susceptibility ($\chi_{rt} = 2 \times 10^{-4}$ emu mol^{-1}) is almost constant down to around 150 K.

Good quality black needle-like single crystals of [BDTFP]₂[PF₆][PhCl]₀.₅ and [BDTFP]₂[AsF₆][PhCl]₀.₅ were grown by conventional electrochemical oxidation in chlorobenzene containing 10% v/v of ethanol. The PF₆ and AsF₆ salts showed room temperature conductivities of 40 and 4.0 S cm^{-1}, respectively. Very small activation energies of $E_a = 0.076$ for the PF₆ salt (at 300–180 K) and 0.078 eV for the AsF₆ salt (at 300–230 K) were obtained from the Arrhenius plots of temperature dependence of the resistivity. Quite interestingly a phase transition was observed at 175 K (Fig. 1 (a)) and 220 K for the PF₆ and AsF₆ salts, respectively. In order to obtain further information on the phase transition, the temperature dependence of the static magnetic susceptibility of the PF₆ salt was measured by the SQUID method. As shown in Fig. 1 (b), the magnetic susceptibility of the PF₆ salt is almost constant from 300 K down to 175 K which is regarded as Pauli paramagnetism, and decreased drastically at 175 K with the transition to a diamagnetic phase. Fig. 2 shows a band structure and the Fermi surface of the PF₆ salt calculated by the tight-binding approximation method using the overlap integrals given in Table 1 (mentioned later). The PF₆ salt has a metallic band structure, since the upper band is half-filled and has an one-dimensional Fermi surface consisting of two pairs of linear planes opening out into the *b*-direction. Therefore, this salt may be metallic above or near 300 K along the stacking *c*-axis. In the temperature region of 300 to 175 K, the metallic phase becomes unstable probably due to the growth of the $4k_F$ CDW (charge density wave), in which the freedom of the spin still remains. Thus, the magnetic phase transition at 175 K appears to be caused by a spin–Peierls transition.

The X-ray crystallographic analysis‡ disclosed that the PF₆ and AsF₆ salts are isomorphous with each other. The unit cell contains four donors and two anions demonstrating that the donor to anion ratio is 2:1; therefore, the formal charge on a donor is +0.5. There are two crystallographically independent donor molecules (A and B) which stack along the *c*-axis in an ABAB manner in two-fold period repetition directing the pyrazine ring to the same side of the molecules (Fig. 3 (b), (c)). The interplanar distances in the columns are 3.47–3.48 Å. Interestingly, the intramolecular N⋯S distances (3.21–3.15 Å) are far shorter than the van der Waals distance (3.35 Å) in both A and B. As a result of the intramolecular N⋯S contacts, both of the donor molecules A and B retain good coplanar conformations with deviation less than 0.1 Å from the optimal plane. The overlapping modes are so-

called ring-over-bond type with slip distances of 1.4 ($c1$) and 1.3 Å ($c2$) along the C–O bond of the furoquinonoid ring (Fig. 4). The pyrazine rings in neighboring columns I and II are directed in opposite directions (Fig. 3 (a)). The PF_6 anions are located in the openings between the donor columns and the chlorobenzene layer separates the donor sheets in the bc plane. Looking for intercolumn interactions, there are some S···S contacts (3.23–3.54 Å) less than the van der Waals distance (3.6 Å) between the columns I and II (and between columns I′ and II′) in which the 1,3-dithiole rings in neighboring columns come close to each other. On the other hand, there is no side-by-side intercolumn contact between columns II and I′, in which the pyrazine rings approach each other closely. Actually, there exists a fairly large intercolumn overlap integral p between columns I and II (Table 1). In contrast, overlap integrals, b, q, q' between columns II and I′ are less than one-tenth of p. Thus it gives rise to the uncommon two-leg ladder type orbital overlapping structure, where the legs of the ladder are the stacking columns I and II (I′ and II′) and the rungs of the ladder correspond to the inter-column overlap integrals, p and a, which are mainly attributed to the effective S···S orbital overlaps indicated in the dotted lines in Fig. 3 (a).§ It is also noticeable that the absolute values of the inter-dimer overlap integral, $c2$ on the leg and the overlap integral, p on the rung are of almost similar magnitude. Ladder materials of interest are those in which the exchange coupling along the rung, $J_\perp$ and the exchange coupling along the leg, $J_{//}$ are of similar magnitude,[6] namely, $0.1 \leqslant J_\perp/J_{//} \leqslant 10$. Judging from the overlap integrals listed in Table 1,¶ our system will be surely within the range. Moreover, one ladder consisting of columns I and II is well isolated from another, since the interladder overlap integrals b, q, q' are less than one-tenth of the intraladder overlap integral, p as mentioned above. Although copper oxide based ladder materials are currently the object of theoretical and experimental investigations in connection with the discovery of high-temperature superconductivity in lightly doped ladder-like antiferromagnets,[7] only a few examples of molecular spin ladder systems are known so far.[6b] Thus detailed investigation of the low temperature electronic states of the PF_6 and AsF_6 salts is needed from the physical view point to elucidate whether a $S = 1/2$ Heisenberg antiferromagnetic spin ladder configuration is really attained in this novel ladder type π-overlapping system based on BDTFP.

Notes and References

†Selected data for BDTFP (1): mp 238 °C (decomp); ^{1}H NMR (600 MHz, C_6D_6), δ 5.45 (d, J 6.3 Hz, 2H, SCHCHS), 5.57 (d, J 6.3 Hz, 2H, SCHCHS), 7.72 (s, 2H, NCHCHN); ^{13}C NMR (150 MHz, C_6D_6), δ 116.1, 117.0, 120.1, 135.3, 140.6, 145.4; IR (KBr) ν 3049, 1610, 1510, 1338, 1161, 1147, 1076, 850, 694 cm^{-1}. UV-vis (THF) λ_{max} (log ε) 570 (sh, 3.83), 528 (3.91), 463 (4.46), 434 (sh, 4.32), 362 (3.99), 340 nm (sh, 3.91); MS (70 eV) : m/z (%) 324 ($M^+ + 2$, 18), 323 ($M^+ + 1$, 18), 322 (M^+, 89), 279 (34), 268 ($M^+ - C_2H_2N_2$, 31) and 149 (100); HRMS: m/z 321.9361 (M^+), calcd for $C_{12}H_6N_2OS_4$: 321.9363.

‡Crystal data for [BDTFP]$_2$[PF$_6$][PhCl]$_{0.5}$: $C_{24}H_{12}N_4O_2S_8PF_6(C_6H_5Cl)_{0.5}$, $M = 846.16$, triclinic space group $P\bar{1}$ (#2), $a = 15.60(1)$, $b = 16.323(10)$, $c = 6.96(1)$ Å, $\alpha = 103.94(8)°$, $\beta = 103.98(8)°$, $\gamma = 95.77(6)°$, $V = 1645(3)$ Å^3, $Z = 2$, $D_c = 1.709$ g cm^{-3}. The final results: R (R_w) = 0.068 (0.079) for 2385 observed ($[I > 4.00\sigma(I)]$) reflections. For [BDTFP]$_2$[AsF$_6$][PhCl]$_{0.5}$: $C_{24}H_{12}N_4O_2S_8AsF_6(C_6H_5Cl)_{0.5}$, $M = 890.11$, triclinic space group $P\bar{1}$ (#2), $a = 15.66(2)$, $b = 16.531(10)$, $c = 6.980(3)$ Å, $\alpha = 104.21(8)°$, $\beta = 102.92(3)°$, $\gamma = 96.42(5)°$, $V = 1681(2)$ Å^3, $Z = 2$, $D_c = 1.759$ g cm^{-3}. The final results: R (R_w) = 0.078 (0.088) for 1749 observed ($[I > 3.90\sigma(I)]$) reflections. The diffraction data were collected using a Raxis II area detector with graphite monochromated Mo-Kα radiation using the ω scan technique ($2\theta < 60.1°$ for the PF$_6$ salt and $2\theta < 60.2°$ for the AsF$_6$ salt). The structure was solved by direct methods (SHELXS86) and was refined by full-matrix least squares analysis.[8] The non-hydrogen atoms were refined anisotropically. All calculations were performed using the teXsan crystallographic software package of MSC.[9] Atomic coordinates, bond lengths and angles, and thermal parameters have been deposited with the Cambridge Crystallographic Data Centre: CCDC 1145/266. See http://www.rsc.org/suppdata/jm/b0/b008758k/ for crystallographic data in cif format.

§The overlap integral p' diagonally connecting the dimers in the legs may affect the frustration effect for the spin–ladder type antiferromagnetic interaction if each dimer carries one localized electron. However, p' will decrease and, on the contrary, p and a will increase when the degree of the dimerization becomes strong at low temperature.

¶Exchange coupling energy, J is proportional to the corresponding transfer integral t as given in the equation: $J = 2t^2/U$ where U is on-site Coulomb energy. The transfer integral t is proportional to the overlap integral s as given in the equation: $t = Es$ where E is constant.

1   M. R. Bryce, J. Chem. Soc., Perkin Trans. 1, 1985, 1675; K. Takahashi, T. Shirahata and K. Tomitani, J. Mater. Chem., 1997, 7, 2375 and references cited therein.
2   H. Yamochi, K. Komatsu, N. Matsukawa, G. Saito, T. Mori, M. Kusunoki and K. Sakaguchi, J. Am. Chem. Soc., 1993, 115, 11319.
3   K. Takahashi, T. Nihira and K. Tomitani, J. Chem. Soc., Chem. Commun., 1993, 1617; K. Takahashi and K. Tomitani, J. Chem. Soc., Chem. Commun., 1995, 821.
4   G. C. Papavassiliou, S. Y. Yiannopoulos and J. S. Zambounis, Chem. Scr., 1987, 27, 265.
5   S. Gabriel and A. Sonn, Chem. Ber., 1907, 40, 4851.
6   (a) E. Dagotto, J. Riera and D. J. Scalapino, Phys. Rev. B, 1992, 45, 5744; (b) C. Rovira, Chem. Eur. J., 2000, 6, 1723.
7   M. Uehara, T. Nagata, J. Akimitsu, H. Takahashi, N. Mori and K. Kinoshita, J. Phys. Soc. Jpn., 1996, 65, 2764.
8   SHELX86: G. M. Sheldrick, in Crystallographic Computing 3, 1985, eds. G. M. Sheldrick, C. Kruger and R. Goddard, Oxford University Press, pp. 175–189
9   teXsan: Crystal Structure Analysis Package, Molecular Structure Corporation, 1985 and 1992..